This article was downloaded by: [University of Kiel]
On: 23 October 2014, At: 06:24
Publisher: Taylor & Francis
Informa Ltd Registered in England and Wales Registered Number: 1072954 Registered office: Mortimer House, 37-41 Mortimer Street, London W1T 3JH, UK

Philosophical Magazine
Publication details, including instructions for authors and subscription information:
http://www.tandfonline.com/loi/tphm19

The core structure of ½(111) screw dislocations in b.c.c. crystals

V. Vítek [a d], R. C. Perrin [b] & D. K. Bowen [c]
[a] Department of Metallurgy, University of Oxford
[b] Theoretical Physics Division, A.E.R.E., Harwell, Berks
[c] School of Engineering Science, University of Warwick, Coventry
[d] Institute of Physics, Czechoslovak Academy of Sciences, Prague
Published online: 13 Sep 2006.

To cite this article: V. Vítek, R. C. Perrin & D. K. Bowen (1970) The core structure of ½(111) screw dislocations in b.c.c. crystals, Philosophical Magazine, 21:173, 1049-1073, DOI: 10.1080/14786437008238490

To link to this article: http://dx.doi.org/10.1080/14786437008238490

PLEASE SCROLL DOWN FOR ARTICLE

Taylor & Francis makes every effort to ensure the accuracy of all the information (the "Content") contained in the publications on our platform. However, Taylor & Francis, our agents, and our licensors make no representations or warranties whatsoever as to the accuracy, completeness, or suitability for any purpose of the Content. Any opinions and views expressed in this publication are the opinions and views of the authors, and are not the views of or endorsed by Taylor & Francis. The accuracy of the Content should not be relied upon and should be independently verified with primary sources of information. Taylor and Francis shall not be liable for any losses, actions, claims, proceedings, demands, costs, expenses, damages, and other liabilities whatsoever or howsoever caused arising directly or indirectly in connection with, in relation to or arising out of the use of the Content.

This article may be used for research, teaching, and private study purposes. Any substantial or systematic reproduction, redistribution, reselling, loan, sub-licensing, systematic supply, or distribution in any form to anyone is expressly forbidden. Terms & Conditions of access and use can be found at http://www.tandfonline.com/page/terms-and-conditions

The Core Structure of $\frac{1}{2}\langle 111\rangle$ Screw Dislocations in B.C.C. Crystals

By V. Vítek
Department of Metallurgy, University of Oxford†
R. C. Perrin
Theoretical Physics Division, A.E.R.E., Harwell, Berks.
and D. K. Bowen
School of Engineering Science, University of Warwick, Coventry

[Received 17 January 1970 and after revision 2 February 1970]

Abstract

A relaxation-type calculation of the structure of the dislocation core has been made for the $\frac{1}{2}\langle 111\rangle$ screw dislocation in b.c.c. crystals, using a variety of central-force potentials. Two stable configurations were found, corresponding to the centre of the dislocation being along either the left-hand or the right-hand type of three-fold screw axis in the crystal. These two configurations differed only in the very centre. For both configurations and for all potentials, the core structure possessed three-fold symmetry, the largest displacements being in the directions in which displacements on {211} type planes were in the twinning sense. The structure can be described by a combination of large displacements on {110} type planes, plus ' stacking faults ', 1–2b wide on {211} type planes in the twinning sense only.

An investigation of the effect of boundary conditions showed that any errors caused by incomplete relaxation were negligible, and that changing the initial dislocation position or the position of the boundaries did not affect the final core structure. Four potentials were used, similar in form but having a five-fold variation in the depth of the minimum. The core structure was similar for all of these : the only changes were in the relative magnitude of the displacements and in the ' stacking fault ' width which varied between, approximately, 1·2b and 2b. This core structure therefore appears to be general for b.c.c. crystals, and the implications of these results on the movement of dislocations are briefly discussed.

§ 1. Introduction

One of the most important factors controlling the movement of dislocations in b.c.c. crystals is believed to be the structure of the dislocation core. This has been emphasized particularly in connection with the study of the temperature dependence of the flow stress, and of the slip geometry, which shows a very characteristic asymmetry connected with the easy and hard glide in the twinning and anti-twinning directions on {211} planes (e.g. Taoka, Takeuchi and Furubayashi 1964,

† On leave from the Institute of Physics, Czechoslovak Academy of Sciences, Prague.

Downloaded by [University of Kiel] at 06:24 23 October 2014

Šesták and Zárubová 1965, Foxall, Duesbery and Hirsch 1967, Bowen, Christian and Taylor 1967). Both these characteristic properties of the plastic deformation of b.c.c. metals appear to be controlled mainly by the movement of $\frac{1}{2}\langle 111\rangle$ screw dislocations, and theoretical explanations based upon dissociation models of the screw dislocation core have been proposed (Hirsch 1960, Escaig 1966, Vítek and Kroupa 1966, Kroupa and Vítek 1967, Duesbery and Hirsch 1968, Duesbery 1969). Originally, stable stacking faults on {110} and {211} planes were suggested on a hard-sphere model or by analogy with twinning (Cohen, Hinton, Lay and Sass 1962, Frank and Nicholas 1953). Screw dislocations with Burgers vector $\mathbf{b}=\frac{1}{2}[111]$ have been assumed to dissociate into sessile form with partials on several {110} and {211} planes of the [111] zone (Sleeswyk 1963, Mitchell, Foxall and Hirsch 1963, Kroupa and Vítek 1964, Foxall *et al.* 1967, Vítek and Kroupa 1968). The motion of a screw dislocation has then been described as a sequence of sessile/glissile transformations and elementary glides on {110} and {211} planes. It has always been found that the theory only fits the experimental data if the width of splitting lies between 1 and $2b$ ($b=|\mathbf{b}|$). It is therefore obvious that the ' splitting ' cannot be taken literally but only as a model of a special core symmetry.

Recently (Vítek 1968), an investigation of the stability of intrinsic stacking faults on {110} and {211} planes in b.c.c. crystals has been made using a more realistic atomic model. Several types of central-force interaction between atoms were assumed, all satisfying the condition that the b.c.c. structure be stable, in particular with respect to some types of deformation. The stacking-fault energy γ, was calculated as a function of the fault vector, $\mathbf{f}$, to give a surface $\gamma(\mathbf{f})$. These ' γ surfaces ' do not possess any local minima for either {110} or {211} planes unless (Eichler and Pegel 1969) the potential is cut off very close to the second-nearest neighbours (which does not seem physically realistic in b.c.c. crystals (Vítek 1970)). It has therefore been concluded that no stable stacking faults can exist on these planes. Nevertheless, it has been shown that dislocations can dissociate, but into partials with ' general ' Burgers vectors and stacking-fault ribbons which are unstable as infinite planar defects (Vítek and Kroupa 1969). Fontaine (1968) proposed that a continuous distribution of partial dislocations should be considered when no stable stacking faults exist. Both these approaches represent a description of the dislocation core ; however, some assumptions must always be made—e.g. the planes of splitting and the number of partials —and it is impossible on this approach to determine the real structure of the core.

In this paper we present the results of a computer simulation of a b.c.c. crystal containing a $\frac{1}{2}\langle 111\rangle$ screw dislocation. In the calculation, a block of discrete crystal lattice is chosen and the anisotropic elastic displacements which would be caused by a screw dislocation in the middle of the block applied to the boundary atoms. Central forces,

Downloaded by [University of Kiel] at 06:24 23 October 2014

similar to those suggested by Johnson (1964) and truncated to second-nearest neighbours are used to describe the interaction between the atoms. The atoms of the crystallite are then relaxed, by a dynamical method, to obtain a stationary configuration of atoms which shows the core structure.

This type of calculation has already been performed, using similar force laws, by several authors. However, their interpretations differ. Bullough and Perrin (1968 a) found an asymmetric splitting of the dislocation core (see also § 7). Chang (1967) concludes that the core region consists of abrupt shears of **b**/3 on three {110} planes which he believes corresponds to three partials and a stacking-fault ribbon of atomic dimensions. On the other hand, Gehlen, Rosenfield and Hahn (1969) state that the core is very narrow, with no noticeable dissociation. Suzuki (1968) carried out the calculations relaxing the rows of atoms in the [111] direction only as solid rods, and found no dissociation.

In this work the calculations were made for four different interaction potentials of the Johnson type (splined polynomial). These were chosen to give a decreasing sequence of stacking-fault energies (absolute values of γ surfaces) on {110} and {211} planes and also to keep constant all other variables, such as elastic constants and lattice parameter ; thus the effect of the stacking-fault energy on the core structure has been studied. To test the validity of the calculation, the influence of the crystallite size and of the applied boundary conditions on the resulting core configuration was carefully investigated for one potential.

§ 2. Boundary Conditions and Method of Calculation

The block of atoms (crystallite) used was a rectangular parallelepiped bounded by the planes $(\bar{1}\bar{1}2)$, $(\bar{1}10)$ and (111). The crystallite size was usually $8a[\bar{1}10]\times 4a[\bar{1}\bar{1}2]\times a/2[111]$, i.e. $8\times 8\times 3$ atoms (fig. 1) ; sometimes crystallites $12\times 12\times 3$ atoms or $16\times 16\times 3$ atoms were used. When a screw dislocation is introduced into the crystallite the periodicity in the [111] direction is preserved and therefore the block of atoms is made effectively infinite in this direction by application of periodic boundary conditions to the (111) planes.

The atoms in the boundary planes $(\bar{1}\bar{1}2)$ and $(\bar{1}10)$ were subjected to anisotropic elastic displacements given by a $\frac{1}{2}[111]$ screw dislocation in the middle of the crystallite. These displacements were calculated using the method of Stroh (1958), solving the resultant equations numerically. Two types of boundary conditions were applied—fixed and flexible.

The fixed boundary conditions mean that the boundary atoms are held rigidly in their dislocated positions and are not allowed to move during the relaxation.

In the case of flexible boundary conditions the crystallite is taken as a set of atoms inside an infinite crystal which deforms elastically outside the crystallite. The boundary atoms are allowed to move during

Downloaded by [University of Kiel] at 06:24 23 October 2014

relaxation, but they are subjected not only to the forces from the atoms of the crystallite but also to constant spring forces proportional to the displacement of the atoms from their dislocated positions. The spring forces simulate the presence of the neighbouring atoms outside the crystallite. The spring constants were chosen as suggested by Gibson, Goland, Milgram and Vineyard (1960). The application of flexible boundary conditions allows an elastic deformation of the boundary and thus effectively increases the size of the crystallite. The use of flexible boundaries proved essential in other similar calculations, for example on the morphology of interstitial aggregates (Bullough and Perrin 1968 b).

The elastic centre of the dislocation was always made to coincide with one of the axes of three-fold screw symmetry in the perfect lattice, e.g. the triangle marked A in fig. 1 which is a projection of the atoms onto the (111) plane. In this picture, as discussed by Suzuki (1968), triangles of type A represent right-handed screw axes and their mirror images, left-handed axes. In each case the pitch is $\frac{1}{2}[111]$. With the usual sign convention, a screw dislocation of $\mathbf{b} = \frac{1}{2}[111]$ gives a left-handed screw distortion and therefore its introduction to a type A triangle eliminates the screw symmetry of the central three rows of atoms. The three atoms bounding triangle A now lie in the same (111) plane. If we reverse the sign of the Burgers vector we in fact convert the right-handed helix formed by the three rows of atoms into a left-handed helix, since the group of three atoms initially bounding triangle A will no longer lie in adjacent (111) planes : atoms in the planes originally below this triangle will have moved up and these form a left-handed helix. Thus the three central rows of atoms are in the same relative positions as in the ideal lattice : there is merely a change in the hand of the helix. The former position of the dislocation is called ' hard ' and the latter ' easy '. The transition from the easy position into the hard and vice versa, without changing the sign of the Burgers vector, can clearly be achieved by moving the elastic centre of the dislocation into a triangle with the opposite orientation. The easy and hard positions of the dislocation centre could lead to two different core configurations ; this has actually been found in the present work.

The equilibrium configuration of the dislocation core is obtained by allowing the crystallite atoms to relax assuming some interaction forces between them. The relaxation involves the integration of the classical equations of motion for the atoms ; the procedure has been described elsewhere (Bullough and Perrin 1968 a, Gibson *et al.* 1960). At first a suitable time step is chosen, the force on each atom is then evaluated, and the mean velocity of each atom over the time step and hence its position at the end of the time step determined. With a suitable choice of the time step the kinetic energy of the atoms passes through a maximum after a few iterations. At this point the atoms are brought to rest and the iterations restarted until the absolute minimum in the potential energy is attained. At the beginning of the relaxation procedure the atoms were

Downloaded by [University of Kiel] at 06:24 23 October 2014

always put into the dislocated positions given by the anisotropic elastic displacements due to the screw dislocation.

Fig. 1

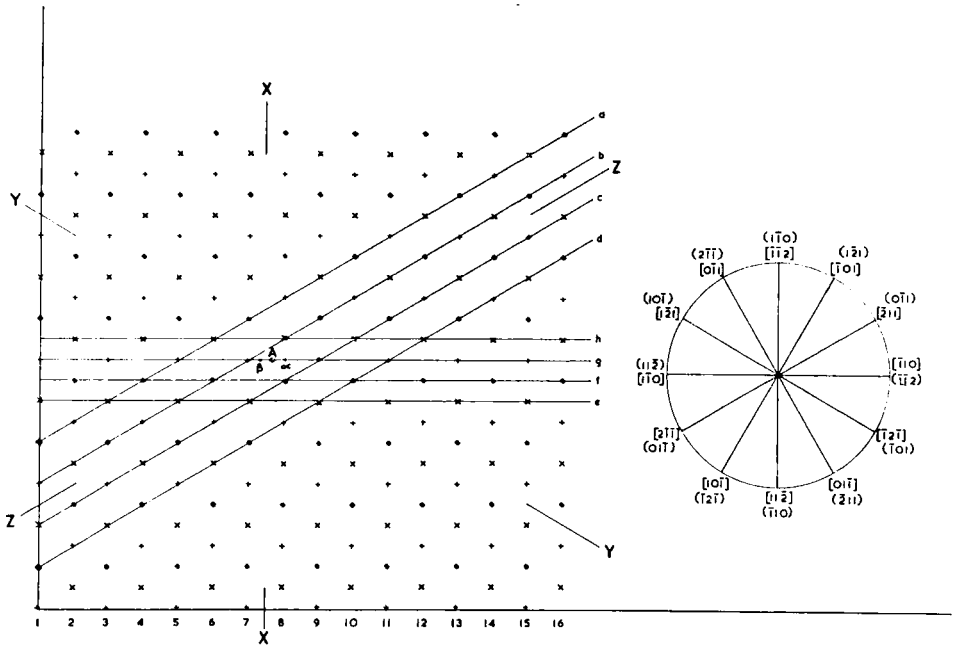

The geometry and crystallography of the atomic model.

§ 3. Interatomic Forces

The present knowledge of interatomic forces, particularly in b.c.c. transition metals, is very limited. We have not, therefore, attempted to make calculations for any particular metal, but rather to study a general b.c.c. crystal. The interaction between atoms has been approximated by central forces such that, at least within limits, the stability of the b.c.c. structure is ensured. The requirements are (Vítek 1968) :

(i) The structure is stable with respect to small deformations (Born and Huang 1954).

(ii) The structure is stable with respect to a large homogeneous expansion or contraction.

(iii) The structure is stable with respect to large displacements on {110} and {211} planes, i.e. the stacking-fault energy on these planes is always positive.

The interaction has been limited to second-nearest neighbours : this is the minimum truncation for which a stable b.c.c. structure can be obtained using purely central-force interactions.

Downloaded by [University of Kiel] at 06:24 23 October 2014

Four central-force potentials $\phi(r)$ have been used, where $\phi(r)$ is the interaction energy at an atomic separation of r. These gave the same lattice parameter and elastic constants but gradually decreasing stacking-fault energy (height of γ surface). For computational convenience we chose the polynomial type of potential suggested by Johnson (1964). Since any potential contains a number of arbitrary constants, only three of which are fixed by the elastic constants, it was possible to vary the stacking-fault energy without altering the elastic constants. The elastic displacements of the dislocation, far from the core, are then the same in all cases ; thus the effect of the stacking-fault energy on the dislocation core alone can be followed. The elastic constants are those used by Johnson, i.e. those which fulfil the Cauchy relations and are derived from those for α-iron. They are $c_{11}=1{\cdot}2$, $c_{12}=0{\cdot}6$, $c_{44}=0{\cdot}6$ in ev Å^{-3}. It is convenient, though not essential, to use constants which fulfil the

The coefficients of the potential J_0 (a_n) and of the potentials J_1, J_2, J_3 (b_n)

	a_1	a_2	a_3	a_4
$r \leqslant 2{\cdot}44$ Å	$-2{\cdot}195976$	$3{\cdot}097910$	$2{\cdot}704060$	$-7{\cdot}436448$
$2{\cdot}44 < r \leqslant 3{\cdot}00$ Å	$-0{\cdot}639230$	$3{\cdot}115829$	$0{\cdot}477871$	$-1{\cdot}581570$
$3{\cdot}00 < r \leqslant 3{\cdot}44$ Å	$-1{\cdot}115035$	$3{\cdot}066403$	$0{\cdot}466892$	$-1{\cdot}547967$

$r \leqslant 2{\cdot}45$ Å	J_1	J_2	J_3
b_0	$5{\cdot}38791474378\times10^{1}$	$1{\cdot}09145106024\times10^{2}$	$1{\cdot}36733632830\times10^{2}$
b_1	$-7{\cdot}43547725438\times10^{1}$	$-1{\cdot}87606578259\times10^{2}$	$-2{\cdot}44152251912\times10^{2}$
b_2	$3{\cdot}89954160672\times10^{1}$	$1{\cdot}22642043930\times10^{2}$	$1{\cdot}64411498390\times10^{2}$
b_3	$-9{\cdot}31287173869$	$-3{\cdot}60227297553\times10^{1}$	$-4{\cdot}93617134566\times10^{1}$
b_4	$8{\cdot}62218341539\times10^{-1}$	$3{\cdot}99723402011$	$5{\cdot}56298318868$
b_5	0	0	0
$2{\cdot}45 < r \leqslant 2{\cdot}90$ Å			
b_0	$9{\cdot}04795451820\times10^{2}$	$1{\cdot}76829052395\times10^{3}$	$2{\cdot}20003800642\times10^{3}$
b_1	$-1{\cdot}64904039436\times10^{3}$	$-3{\cdot}25687077355\times10^{3}$	$-4{\cdot}06078596316\times10^{3}$
b_2	$1{\cdot}20190756191\times10^{3}$	$2{\cdot}39684643149\times10^{3}$	$2{\cdot}99431586627\times10^{3}$
b_3	$-4{\cdot}37870691658\times10^{2}$	$-8{\cdot}80977197181\times10^{2}$	$-1{\cdot}10253044994\times10^{3}$
b_4	$7{\cdot}97144623525\times10^{1}$	$1{\cdot}61708518067\times10^{2}$	$2{\cdot}02705545925\times10^{2}$
b_5	$-5{\cdot}79945932381$	$-1{\cdot}18573787925\times10^{1}$	$-1{\cdot}48863385267\times10^{1}$
$2{\cdot}90 < r \leqslant 3{\cdot}44$ Å			
b_0	$1{\cdot}34355108792\times10^{2}$	$1{\cdot}05433460188\times10^{2}$	$9{\cdot}08055082776\times10^{1}$
b_1	$-1{\cdot}69677011742\times10^{2}$	$-1{\cdot}33905651420\times10^{2}$	$-1{\cdot}15800983508\times10^{2}$
b_2	$7{\cdot}97488087867\times10^{1}$	$6{\cdot}33459782526\times10^{1}$	$5{\cdot}50372205724\times10^{1}$
b_3	$-1{\cdot}65518219235\times10^{1}$	$-1{\cdot}32419908438\times10^{1}$	$-1{\cdot}15637614366\times10^{1}$
b_4	$1{\cdot}28113797562$	$1{\cdot}03289469100$	$9{\cdot}06880693150\times10^{-1}$
b_5	0	0	0

Downloaded by [University of Kiel] at 06:24 23 October 2014

Cauchy relations in this type of calculation. The lattice constant for α-iron, $a = 2{\cdot}86$ Å has been used throughout. These parameters were chosen only because the first of the potentials, J_0, is the original Johnson potential

$$\phi(r) = a_1(r-a_2)^3 + a_3 r + a_4$$

for $r \leqslant 3{\cdot}44$ Å and $\phi(r) = 0$ for $r > 3{\cdot}44$ Å. The other potentials, J_1, J_2, J_3 (which are not the same as those used in Vítek (1968) as only stacking faults lower in energy than that given for J_0 were investigated), are expressed in the polynomial form

$$\phi(r) = \sum_{n=0}^{n=5} b_n r^n$$

for $r \leqslant 3{\cdot}44$ Å and $\phi(r) = 0$ for $r > 3{\cdot}44$ Å.

The coefficients a_n and b_n are given in the table. The potentials are shown in fig. 2. In fig. 3 we show the cross sections of the γ surface for the (112) plane in the $[\bar{1}\bar{1}1]$ direction, calculated as in Vítek (1968); the stacking-fault vector $\mathbf{f} = x/2[\bar{1}\bar{1}1] + y/2[1\bar{1}0]$, where $0 \leqslant x \leqslant 1$, $0 \leqslant y \leqslant 1$ and the cross sections are for $y = 0$. The curves do not possess any minima, which means that there are no stable stacking faults, but they show the asymmetry connected with the twinning and anti-twinning directions of the shift on these planes.

Fig. 2

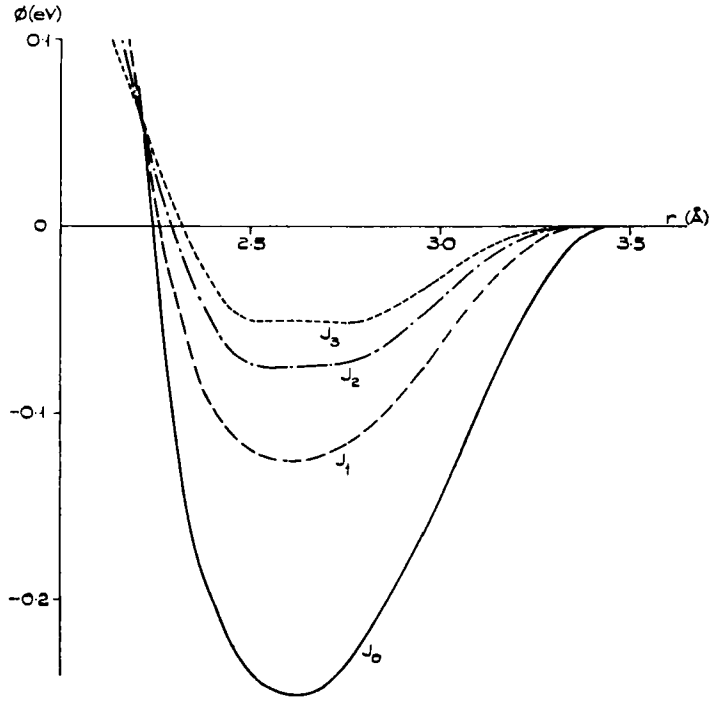

The interatomic potentials, J_0–J_3.

Downloaded by [University of Kiel] at 06:24 23 October 2014

Fig. 3

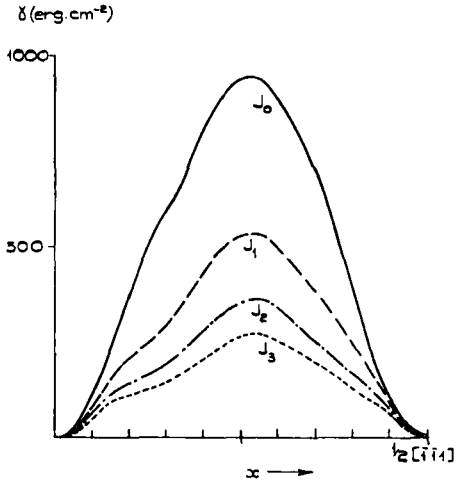

Cross sections of the γ surfaces on the (112) plane in the $[\bar{1}\bar{1}1]$ direction for the four potentials.

§ 4. The Structure of the Dislocation Core

In this section we present the interpretation of the calculations and discuss in detail the structure of the dislocation core. The necessary geometry and crystallography are shown in fig. 1 ; this is an orthogonal projection on to (111) of the atoms in a rectangular b.c.c. crystal whose dimensions are $8 \times 8 \times 3$ atoms in the $[1\bar{1}0]$, $[\bar{1}\bar{1}2]$ and [111] directions respectively. The stacking sequence ABCABC is represented by atomic symbols in the order $+ \blacklozenge \times$ in the positive [111] direction (out of the paper).

We shall discuss the method of interpretation for the potential J_2 since this was used for investigating the effects of the boundary conditions and crystallite size upon the relaxation ; moreover the core structure is best visible for this potential, especially for the hard configuration. As shown in § 5, the calculation with flexible boundary conditions for an $8 \times 8 \times 3$ crystallite was found to be satisfactorily relaxed. The displacements in the [111] direction around the dislocation in the ' hard ' position are shown in figs. 4 (*a*) and 4 (*b*). We use ' displacement ' in this paper to mean the displacement caused solely by the dislocation : the displacement between two atoms is therefore the difference between the vector connecting the atoms in the dislocated crystal and that connecting them in the perfect crystal. In fig. 4 and subsequent pictures of the same type (' displacement maps ') we plot the [111] component of the displacement between two atoms as an arrow pointing from one of the atoms to the other, in the projection on to (111), centred on the mid-point of the two atoms. The dislocated atomic coordinates are used

Downloaded by [University of Kiel] at 06:24 23 October 2014

Fig. 4

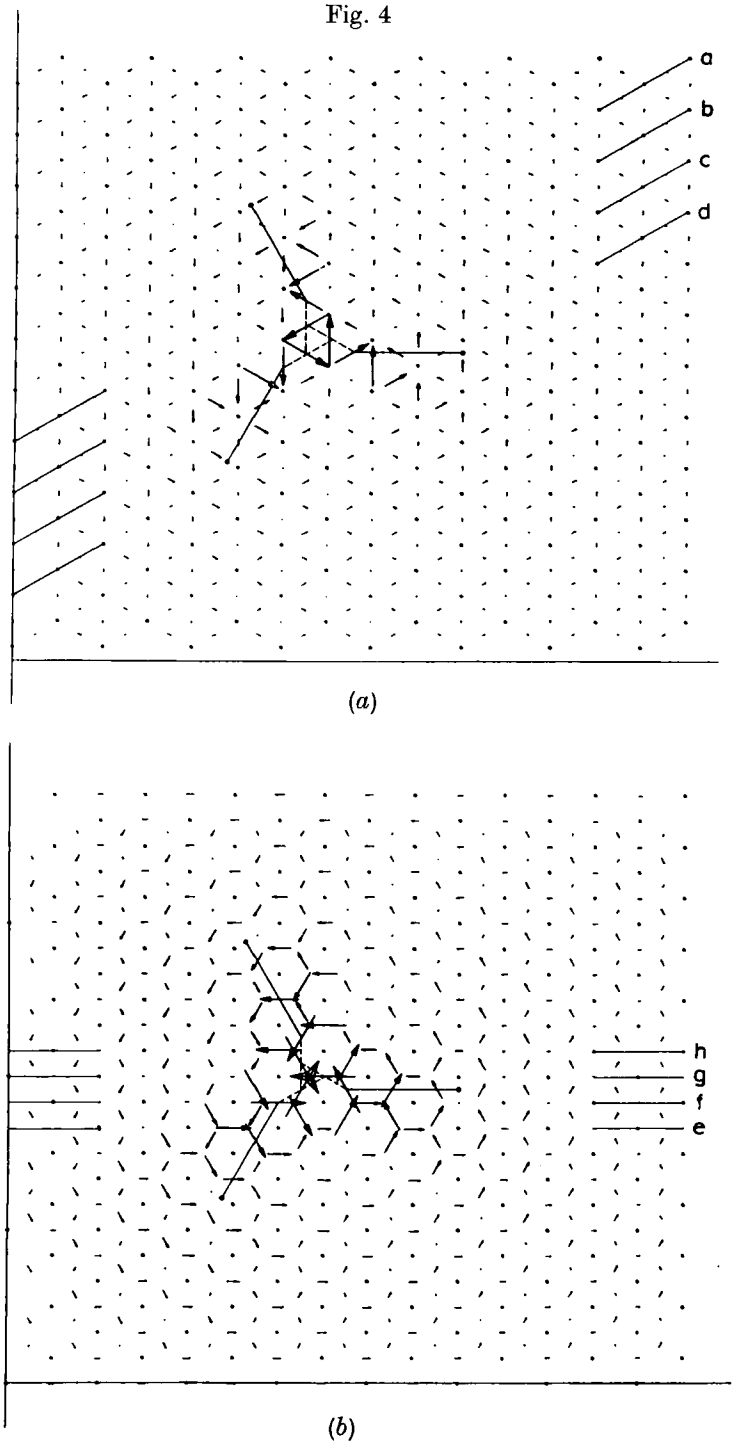

(*a*) {110} displacement maps. (*b*) {211} displacement maps for the potential J_2, hard configuration. The interpretation of the configuration is also shown.

Downloaded by [University of Kiel] at 06:24 23 October 2014

to find the mid-points and directions of the arrows, but the undislocated atomic coordinates in the projection are shown as dots (without distinction of [111] coordinate). Thus the arrows all represent the displacements in the [111] direction, and their deviations from the centre and direction of the line connecting corresponding atoms in the projection show the displacements perpendicular to [111]. The latter displacements were always very small. For clarity we plot separately the displacements between adjacent atoms in the three {110} planes (fig. 4 (*a*)) and in the three {211} planes (fig. 4 (*b*)) which lie in the [111] zone.

In all cases the scale of the arrows is such that a displacement of $|\frac{1}{6}[111]|$ is put equal to $|\frac{1}{2}[211]|$ on the plot. The absolute direction of the arrows gives the sign of the displacement : the arrows therefore reverse in identical planes on either side of the dislocation core, as in the $(01\bar{1})$ planes marked *b* and *c* in fig. 4 (*a*). The actual atomic positions in the four $(01\bar{1})$ planes marked *a*–*d* in figs. 1 and 4 (*a*) are shown in fig. 5 : the numbering of the atoms corresponds to the numbering of atomic rows in fig. 1. By looking along atomic rows in the $[\bar{1}11]$ direction the displacements may be seen directly, and may be correlated with the arrows in fig. 4 (*a*).

The dotted and solid lines in the centre of figs. 4 (*a*) and 4 (*b*) represent an interpretation of the displacements which we shall discuss shortly. We may deduce directly from the displacement maps alone that

(i) the displacements possess three-fold symmetry about the centre of the dislocation (i.e. about the three-fold screw symmetry axis). The three central atoms are displaced by just $\frac{1}{6}[111]$ as discussed in § 2, so that they are now in the same {110} plane ;

(ii) there are large displacements on the three {110} planes radiating directly from the centre, i.e. planes XX, YY, and ZZ in fig. 1, and on these planes the displacements decrease monotonically with distance from the centre (we shall refer to these planes as the ' {110} misfit planes '). These displacements correspond to the dislocation having a finite ' width ', but it is important to note that they are largely confined to just three planes. Moreover, the displacements on any one of these planes are much larger on one side of the dislocation centre than on the other ; this is not expected from the symmetry of {110} planes ;

(iii) displacements in regions other than on the {110} misfit planes do not show reflection symmetry about these planes even though {110} planes are mirror symmetry planes of the crystal (strictly, the XX, YY, and ZZ planes lie between the atoms and in crystallographic notation are glide planes). The displacements are considerably larger on those sides of the {110} misfit planes on which we have drawn solid lines, than on the other sides. The solid lines are drawn on {211} type planes, on that side of the centre on which displacements are in the twinning sense on these planes. Examination of the displacements across these planes shows that they are much larger than on any other plane except the three {110} misfit planes.

Downloaded by [University of Kiel] at 06:24 23 October 2014

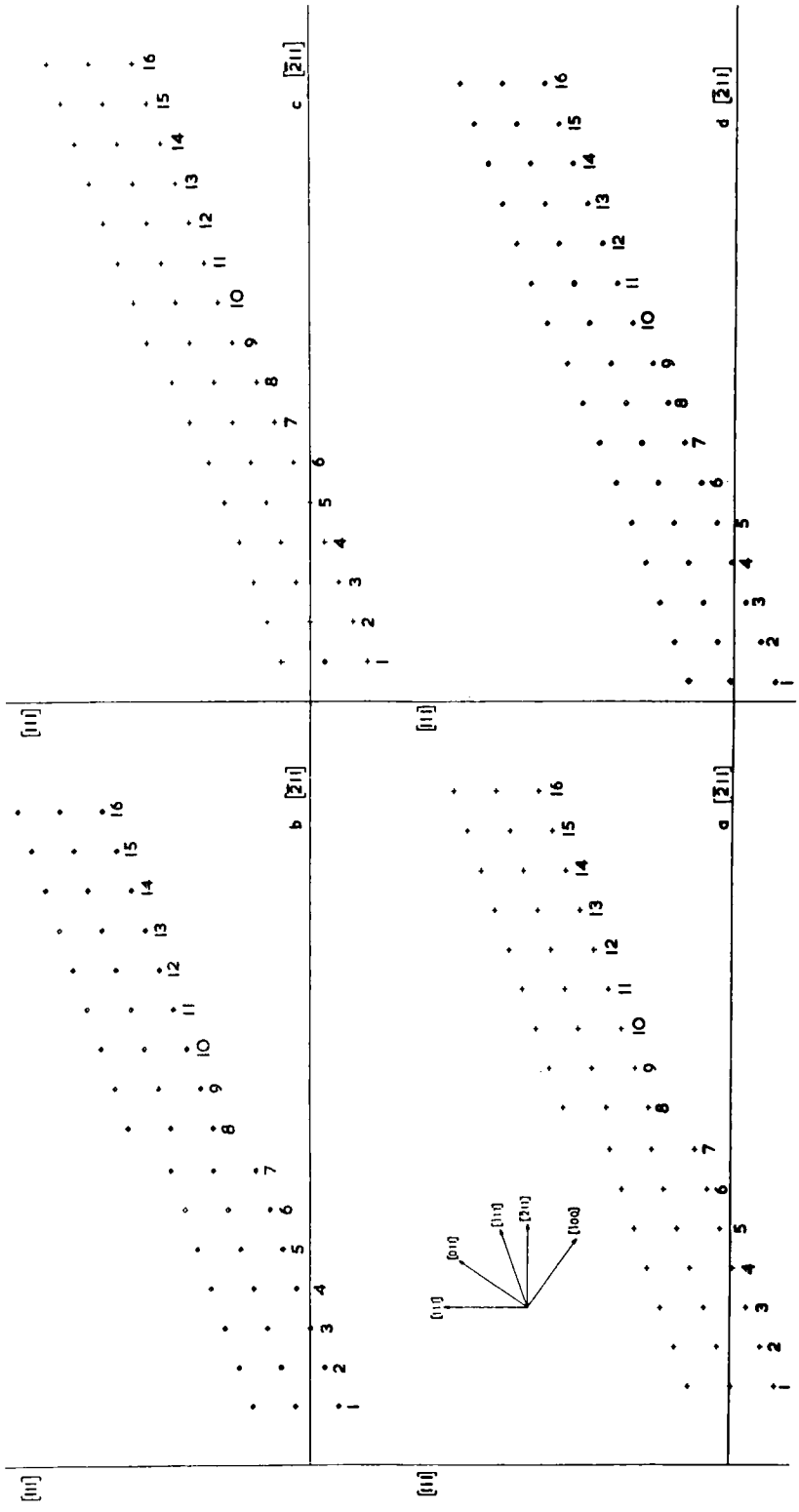

Fig. 5

Sequence of $(01\bar{1})$ planes marked *a*, *b*, *c*, *d* in fig. 1. The numbering corresponds to the numbering of atomic rows in fig. 1.

Downloaded by [University of Kiel] at 06:24 23 October 2014

The results of the calculations are therefore that the displacements are concentrated on six planes, three {110} and three {211}. Displacements on the {211} planes are only large when in the ' twinning sense ' of shear. The displacements on the {110} planes are much larger on that side of the core on which the {211} plane intersected by the appropriate {110} plane is sheared in the twinning sense. Outside a circle of radius approximately $4b$ ($b = |\mathbf{b}|$) the displacements are not significantly concentrated on any particular set of planes.

The question of the relationship between this configuration and earlier models based upon stacking faults and partial dislocations naturally arises. It is clear that the core is too narrow to apply these concepts rigidly, but it is possible to discuss qualitatively the displacements in such terms. In figs. 4 (*a*) and 4 (*b*) we show our interpretation ; the dotted lines represent the region of exact $\frac{1}{6}[111]$ displacements, which we consider to arise purely for reasons of symmetry (§ 2) and the solid lines represent stacking faults on {211} planes in the twinning sense terminated by partials. The {110} misfit planes XX, YY and ZZ are found by producing the dotted lines. The width of the ' stacking-fault ribbons ' is about $2b$. In each case we see large displacements across the faults ; for example, the displacements in plane *c* (fig. 4 (*a*)) show a double maximum, one corresponding to crossing the fault, the other to crossing the plane YY. Plane *d* shows a similar double maximum, the first corresponding to the region of the partial dislocation, but the next $(01\bar{1})$ plane down shows no maximum near the partial dislocation, although the displacements are larger on this side of the misfit plane YY than on the other. It therefore seems reasonable to fix the partial dislocation in the position drawn. In each case we studied all the {110} and {211} planes in the [111] zone (e.g. fig. 5) as well as the {110} and {211} displacement maps, on large-scale pictures, before deciding on the positions for the faults and partials. The actual stacking on the appropriate {211} planes is shown in fig. 6 in which the atomic positions in the four $(\bar{1}\bar{1}2)$ planes marked *e, f, g, h* in figs. 1 and 4 (*b*) are superimposed. Planes *e, f* (–⟨, ⟩–) are below the fault and *g, h* (+, ▱) above it. The centre of the dislocation, the region of the stacking fault and the region of the partial dislocation are marked C, S and P respectively. It is clear that deviations from normal stacking are much greater in region S than on the other side of the centre ; they correspond, in region S, to shear in the twinning sense. The ' fault vector ' is much less than $\frac{1}{6}[111]$, but we cannot determine it exactly since the fault ribbon is so narrow, and overlaps near the core with the displacements on the $(01\bar{1})$ misfit plane.

For the remainder of the paper we shall not discuss the deductions in such detail, but present only the displacement maps and the representation of the core configuration in terms of stacking faults.

The displacement maps and core structure are shown in figs. 7 (*a*) and 7 (*b*) for the easy position of the dislocation. These, and the

Downloaded by [University of Kiel] at 06:24 23 October 2014

remaining displacement maps, are drawn to a larger scale and show only the central part of the crystallite. Again we see displacements of exactly $\frac{1}{6}[111]$ in the central atoms : since they are in the opposite sense, as discussed in § 2, the atoms occupy the same relative positions as in the ideal crystal, with merely a change in the hand of the helix which they form. This is compensated for by further shifts of $\frac{1}{6}[111]$ in the next nearest atoms, as seen in the {110} displacement map (fig. 7 (*a*)). The centre of the dislocation is therefore broader (the $\frac{1}{6}[111]$ displacements are again represented by dotted lines on the {110} misfit planes) but stacking faults and partials are again seen from double maxima in the displacements in the appropriate {110} and {211} planes. The stacking faults again only exist when their shear is in the twinning sense, and although they are one plane further from the centre, their width is the same in both the easy and the hard position, i.e. $\sim 2b$.

Fig. 6

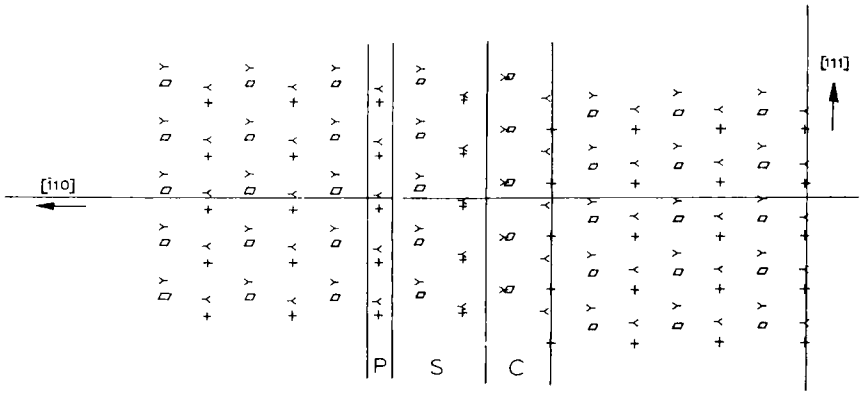

Superimposed sequence of $(\bar{1}\bar{1}2)$ planes marked *e*, *f*, *g*, *h* in fig. 1. C = core region, S = stacking-fault region, P = partial dislocation region.

The large displacements on {110} misfit planes again appear on one side of the core only in each case, the side being determined by the intersection of the misfit plane with the {211} plane sheared in the twinning direction. The misfits on {110} planes are large in the same directions for both $\mathbf{b} = \pm\frac{1}{2}[111]$ although the faults on {211} planes are in the opposite directions (provided the centre of the dislocation is placed in the same type of triangle). If the centre is placed in a triangle of type A (right-hand screw axis, fig. 1) the large displacements on {110} planes are in the $[\bar{1}\bar{1}2]$, $[2\bar{1}\bar{1}]$ and $[\bar{1}2\bar{1}]$ directions for both $\mathbf{b} = \pm\frac{1}{2}[111]$. If a dislocation with $\mathbf{b} = \frac{1}{2}[111]$, say, be moved from this position so that its centre is made to coincide with a left-hand screw symmetry axis (i.e. the centre of a triangle with the opposite orientation to A in fig. 1) it must change from the hard to the easy configuration. It follows that

Downloaded by [University of Kiel] at 06:24 23 October 2014

Fig. 7

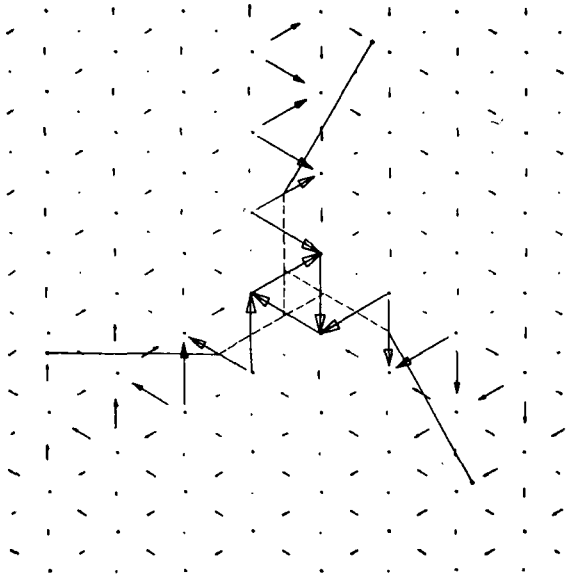

(*a*)

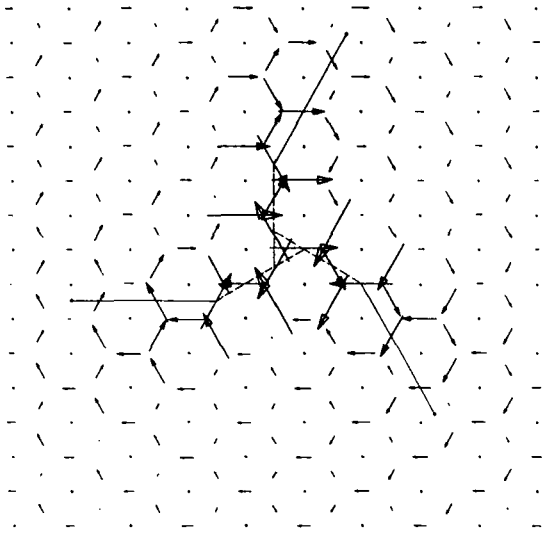

(*b*)

(*a*) {110} displacement maps. (*b*) {211} displacement maps for potential J_2, easy configuration. The interpretation is also shown.

Downloaded by [University of Kiel] at 06:24 23 October 2014

the stacking-fault planes are now on the same side of the core but displaced by two planes. A given {211} fault plane will now intersect a *different* misfit plane, and the large displacements on {110} planes are therefore found on opposite sides of the centre. The four possibilities, $\mathbf{b} = \pm\frac{1}{2}[111]$ and the centre in a right- or left-handed screw axis are shown in fig. 8, in which the large misfits on {110} planes are in each case found on the same side of the centre as the dotted lines representing $\frac{1}{6}[111]$ displacements. We see that, for example, the $(\bar{1}2\bar{1})$ plane intersects misfit plane ZZ, $(01\bar{1})$, in the hard configuration but intersects XX, $(\bar{1}10)$, in the easy configuration.

Fig. 8

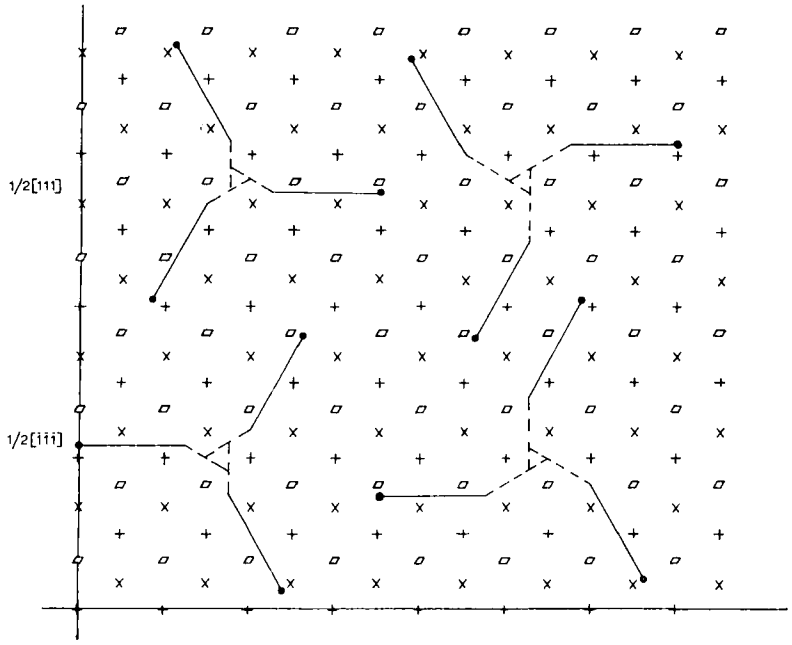

The four possible core configurations, with the two hard configurations on the left and the two easy configurations on the right.

§ 5. Influence of the Crystallite Size and the Boundary Conditions

In order to ascertain that the calculated structure of the dislocation core is not significantly affected by the size of the crystallite nor by the boundary conditions used throughout ($8 \times 8 \times 3$ atoms in the crystallite, flexible boundary conditions) we have made a detailed study of their influence on the relaxation procedure. The potential J_2 was used in this study since a relatively wide core was obtained (see § 6) for this potential and the calculation might therefore have been affected by these constraints.

Downloaded by [University of Kiel] at 06:24 23 October 2014

Fig. 9

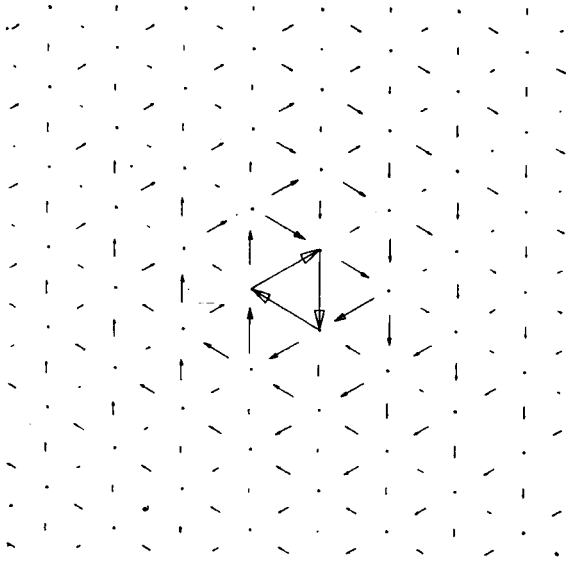

(*a*)

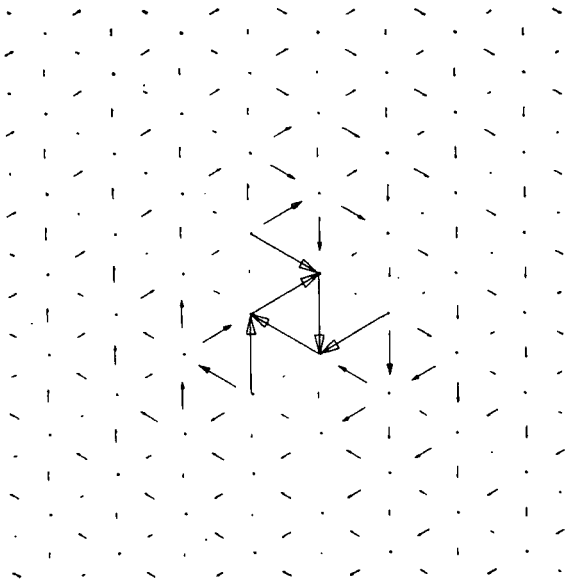

(*b*)

Downloaded by [University of Kiel] at 06:24 23 October 2014

Fig. 9 (*continued*)

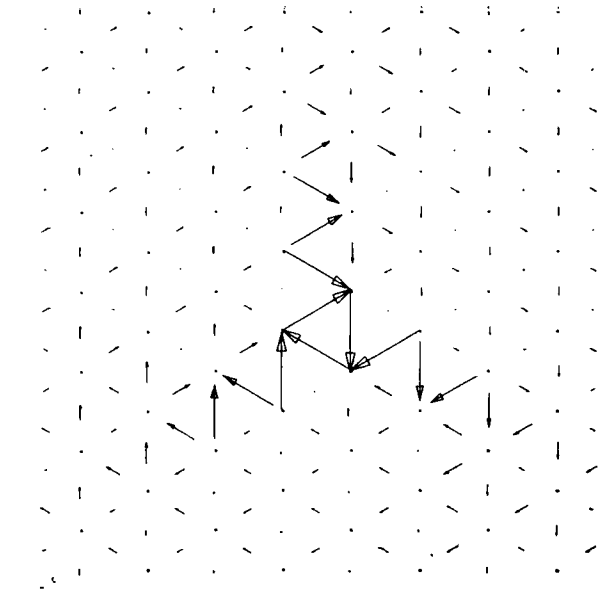

(*c*)

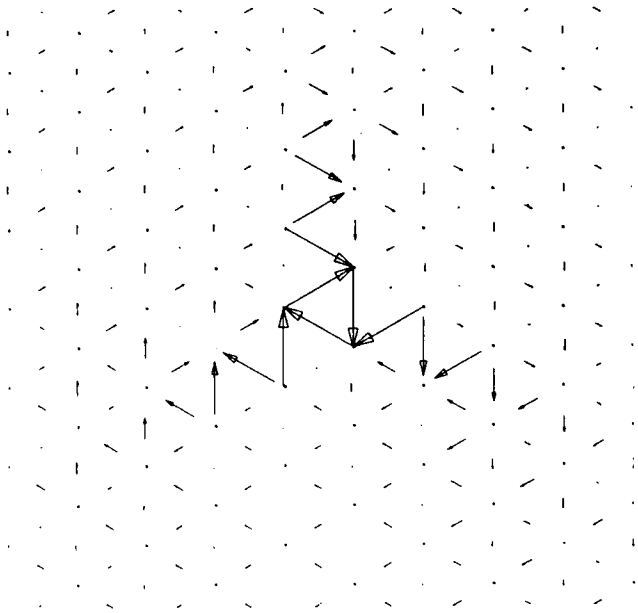

(*d*)

{110} displacement maps, showing effect of boundary conditions for potential J_2, easy configuration. (*a*) $8 \times 8 \times 3$ fixed boundary, (*b*) $12 \times 12 \times 3$ fixed, (*c*) $16 \times 16 \times 3$ fixed, (*d*) $12 \times 12 \times 3$ flexible boundary. Figure 7 (*a*) shows $8 \times 8 \times 3$ flexible boundary.

Downloaded by [University of Kiel] at 06:24 23 October 2014

We must first prove that the choice of conditions at the start of the relaxation does not affect the result : we therefore repeated the calculations using flexible boundary conditions with an $8 \times 8 \times 3$ crystallite, positioning the elastic centre of the dislocation in the positions α and β in triangle A (fig. 1). After relaxation the core structure was always found to be insignificantly different from that found when the centre was initially placed in the centre of triangle A. The core structure therefore is centred on a threefold screw symmetry axis and the displacements show threefold symmetry, regardless of the initial position of the elastic centre.

For the other test calculations we placed the elastic centre of the dislocation in the centre of triangle A, and made $\mathbf{b} = \pm \frac{1}{2}[111]$ to study both easy and hard configurations. The test conditions were (*a*) fixed boundary conditions for crystallite of $8 \times 8 \times 3$, $12 \times 12 \times 3$ and $16 \times 16 \times 3$ atoms and (*b*) flexible boundary conditions (which effectively increase the crystallite size) for $12 \times 12 \times 3$ atoms. The results were examined in detail as described in § 4, and the {110} displacement maps are shown in fig. 9 for the easy configurations, which may be compared with the previous result for $8 \times 8 \times 3$ atoms with flexible boundary conditions shown in fig. 7 (*a*). It is evident from the figures that there is a considerable difference between the $8 \times 8 \times 3$ and $12 \times 12 \times 3$ crystallites with fixed boundary conditions, but a negligible difference between the same size crystallites with flexible boundary conditions. The difference between the $8 \times 8 \times 3$ crystallite with flexible boundary conditions and the $16 \times 16 \times 3$ crystallite with fixed boundaries is also very small, and the characteristic features of the dislocation core described in § 4 are even seen for the $12 \times 12 \times 3$ crystallite with fixed boundary conditions. Only the $8 \times 8 \times 3$ crystallite with fixed boundary conditions is really unsatisfactory. These conclusions have been confirmed by a more detailed analysis of the displacements in all the {110} and {211} planes in the [111] zone for both the easy and hard configurations.

We therefore consider that the configuration obtained for the $8 \times 8 \times 3$ crystallite with flexible boundary conditions is sufficiently close to that which would be obtained for an infinite crystallite. A further increase in the crystallite size would lead only to trivial changes in the core structure but to a great increase in the computing time.

§ 6. Influence of the Magnitude of Interatomic Forces

The core structure has been calculated using four interaction potentials, described in § 2, for both easy and hard configurations (for a crystallite of $8 \times 8 \times 3$ atoms with flexible boundary conditions). The easy configurations for the potentials J_0, J_1 and J_3 are shown on the respective {110} displacement maps in fig. 10 (the same map for the potential J_2 is seen in fig. 7 (*a*)).

The most important result of these calculations is that the overall structure of the dislocation core, for both easy and hard configurations, is the same, regardless of the potential used. The core structure can

Downloaded by [University of Kiel] at 06:24 23 October 2014

Fig. 10

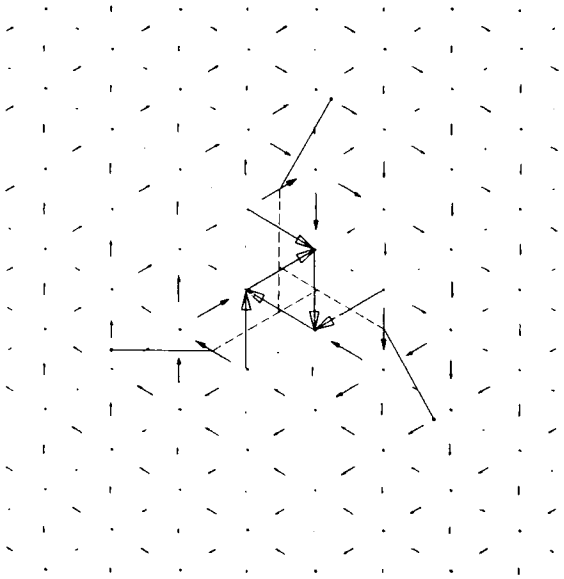

(*a*)

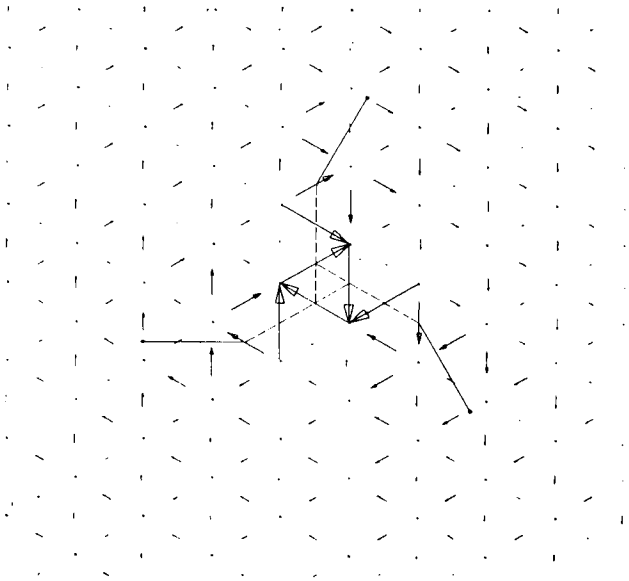

(*b*)

Downloaded by [University of Kiel] at 06:24 23 October 2014

Fig. 10 (*continued*)

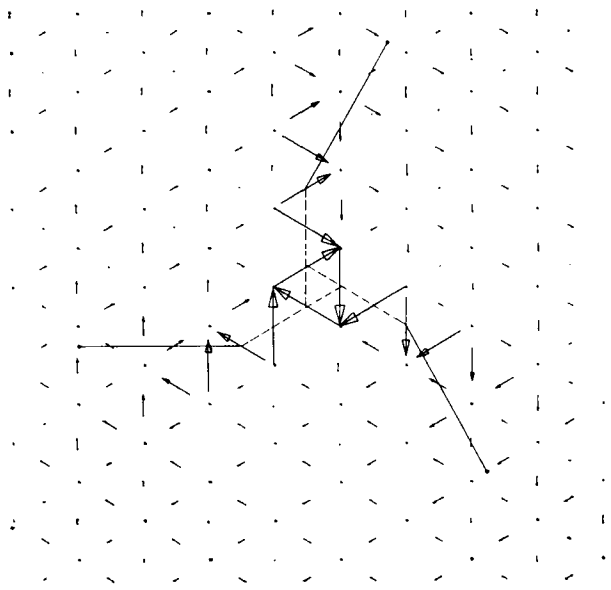

(*c*)

{110} displacement maps showing the effect of the potential, for the easy configuration with 8×8 flexible boundary conditions. (*a*) J_0, (*b*) J_1, (*c*) J_3. Figure 7 (*a*) shows J_2.

always be interpreted in terms of splitting on the three {211} planes in the twinning directions, together with large monotonically decreasing displacements on three {110} planes radiating from the centre. Although the interpretation is less apparent for the potentials J_0 and J_1 than for J_2 and J_3 it is seen that the principal features of the core are the same.

In general the magnitude of interatomic forces influences both the magnitude of the displacements inside the core and its width. If we define, somewhat arbitrarily, the radius of the core to be that distance from the centre of the dislocation beyond which the strain is smaller than 0·1 (i.e. displacements in the [111] direction are smaller than $\frac{1}{60}$ [111]), the core radii are : $3{\cdot}75b$ for J_0, $4b$ for J_1, $4{\cdot}5b$ for J_2 and $5b$ for J_3. They are the same for both easy and hard configurations.

The displacements across {110} and {211} planes appear, however, to behave differently. As discussed previously, the displacements on the two types of plane overlap, so we cannot ascribe a well-defined stacking-fault vector to the faults. This difficulty is not important because the concept of stacking faults is only used to describe those displacements confined to some {211} plane which are responsible for the core asymmetry. As described in § 4 the positions of the partials can be approximately identified

Downloaded by [University of Kiel] at 06:24 23 October 2014

and thus the width of the stacking-fault ribbons defined. Because of the discrete structure of the lattice we can recognize a change in the width of splitting only if it is larger than the distance between successive [111] rows in the corresponding $\langle 110\rangle$ directions on $\{211\}$ planes, which is $b\sqrt{\frac{2}{3}} = 0{\cdot}816b$. We thus take the width to be the same for the potentials J_0 and J_1 ($1{\cdot}2b$) and for the potentials J_2 and J_3 ($2b$), although it might be argued that, e.g., the splitting is less extended in the case of J_0 than in the case of J_1. The width of the stacking fault ribbons is again the same for both easy and hard configurations ; the only difference is in the position of the stacking fault planes.

The width of the large displacements on $\{110\}$ planes radiating from the dislocation centre can be defined as a distance beyond which no maxima in displacements occur when crossing these planes. This distance could also be taken as a definition of the radius of the screw dislocation core. The width, defined in this way, is practically independent of the magnitude of interaction forces ; it is about $4b$ for all the potentials used and for both core configurations.

From this study we see that the width of the displacements on $\{211\}$ planes increases with decreasing stacking-fault energy, which is the usual effect on the width of splitting, whilst the width of the large displacements on $\{110\}$ planes does not change. This fact supports the presented interpretation of the core structure since the displacements on $\{211\}$ planes appear to be of the stacking-fault type.

The total potential energy of the crystallite was also evaluated in the course of our calculations. We deliberately refrain from quoting absolute figures for dislocation core energies since we do not believe that the present knowledge of interatomic forces is sufficiently accurate (§§ 2 and 7). One result however, holds for all the potentials used : the energy of the hard configuration is about 8% higher than that of the easy configuration (which has a less severe distortion at the very centre). It is therefore likely that the easy position is the stable form, although the hard position is certainly in a local potential energy minimum.

§ 7. Discussion

In our calculations of the dislocation core structure we have used a central-force interaction between the atoms of the b.c.c. crystal. This force law is certainly a crude simplification of the real interatomic forces, especially in transition metals. We, therefore, do not suppose that specific properties of a given metal, such as the core energy, can be found in this approximation. On the other hand, we believe that those properties which are general for all b.c.c. metals can be found, provided only that the force law ensures, at least within limits, stability of the b.c.c. structure. Experimental results on the slip geometry (in particular the asymmetry of slip) which is believed to be controlled by the structure of the screw dislocation core, are very similar for many b.c.c. metals and alloys. The slip geometry has been studied for example in silicon-iron (Taoka *et al.*

Downloaded by [University of Kiel] at 06:24 23 October 2014

1964, Šesták and Zárubová 1965, Šesták, Zárubová and Sládek 1967), niobium (Foxall *et al.* 1967, Bowen *et al.* 1967, Duesbery and Foxall 1969), tantalum (Byron and Hull 1967), niobium–molybdenum alloys (Statham 1968) and qualitatively the same behaviour has been found in each system. There are of course quantitative differences. We therefore think that the structure of the screw dislocation core is in principle the same for all b.c.c. metals.

The main features of the $\frac{1}{2}\langle 111\rangle$ screw dislocation core were found to be :

(i) The centre of the dislocation is identical with an axis of three-fold screw symmetry in the perfect crystal.

(ii) The displacements within the core are largely confined to three {110} planes radiating from the dislocation centre and to three {211} planes displaced with respect to the centre as shown, e.g., in figs. 4 and 7.

(iii) The displacements on each of the above {110} planes extend on one side only of the dislocation centre, and decrease monotonically with distance from the centre. The displacements on {211} planes extend in ' twinning directions ' only and do not decrease monotonically. They can be interpreted in terms of stacking faults. The core structure is then described by splitting on three {211} planes in the twinning directions plus large monotonically decreasing displacements on three {110} planes. Since both types of displacement are partially superimposed, the Burgers vectors of the partial dislocations cannot be uniquely determined. They are closely parallel to [111] and (for the outer partials) considerably smaller than $\frac{1}{6}\langle 111\rangle$, the vector usually assumed for partials on {211} planes.

(iv) Two configurations of the core exist, easy and hard. The characteristic features of the core structure are the same for both configurations, and the main differences exist in the very centre ; the centre of the core is broader and the {211} stacking-fault planes farther from the centre for the easy configuration. The easy configuration appears to be energetically about 8% more favourable than the hard position.

We should emphasize that what we really describe in an interpretation of the core structure are anisotropies in the atomic displacements within the core : certain of these anisotropies may be represented by means of stacking faults and partial dislocations. For example, the displacements are always large in those three regions around the core where displacements across {211} planes correspond to shear in the twinning sense. Since the {211} planes are the simplest planes which can show an asymmetry dependent upon the sense of shear, and the displacements across them in our results do not decrease monotonically with distance from the centre, we postulate stacking faults on {211} planes. These faults, however, must not be taken in exactly the same sense as, for example, in f.c.c. crystals, as in no case do we see constant displacements across any plane for a reasonable distance as one would expect for a genuine stacking fault. We must rather treat the displacements across particular {211} planes as stacking-fault type displacements. On the other hand, we could formally

Downloaded by [University of Kiel] at 06:24 23 October 2014

unify the treatment of all the displacements by considering a continuous distribution of partial dislocations (Fontaine 1968), as in the original Peierls model of the core. In this case the distributions on {110} planes would have a monotonically decreasing density with distance from the centre, but on {211} planes the density would not monotonically decrease but may have some other maxima in addition to that at the centre of the total dislocation.

This interpretation differs from that given by Bullough and Perrin (1968 a). In fact the results of the calculation in the earlier work were essentially the same ; however, the particular {211} planes across which the displacements were examined did not reveal the full symmetry of the core.

The core structure shows an asymmetry which can explain the asymmetry of slip. Since the splitting on {211} planes occurs only on the twinning sides of the core, glide should be easier in the twinning than in the anti-twinning direction.

As shown in § 4, the sides of the core on which large displacements on {110} misfit planes occur, are uniquely determined by the intersection of these planes with {211} stacking-fault planes. For a given sign of the Burgers vector those sides can only be reversed when the core configuration changes from easy to hard and vice versa (see fig. 8). If more dislocations exist in the easy configuration than in the hard (and our results indicate that ' easy ' energy is 8% lower) then the large displacements on {110} misfit planes will occur predominantly in one sense. The influence of this on dislocation glide cannot be found in this static study since it depends on the details of the trajectory of the moving dislocation.

The concentration of displacements on three {211} and three {110} planes means that the core is distributed on several non-parallel planes. This can be regarded as a sessile core configuration, which may be compared with former assumptions about sessile splitting of screw dislocations in b.c.c. crystals. The core structure shows a three-fold symmetry, which agrees in principle with the original suggestion of Hirsch (1960) that sessile splitting will possess this symmetry. In this case, splitting was assumed to take place on the three {211} planes in the [111] zone, with partials of $\frac{1}{6}$[111] Burgers vector. However, Sleeswyk (1963) argued that this configuration is unstable, and that a stable splitting is obtained only when one of the partials returns to the centre of the dislocation, which destroys the three-fold symmetry. This argument is valid for large splittings with clearly distinguished partials and stacking-fault ribbons : instability occurs because there is no central partial dislocation. However, if the Burgers vectors of the outer partials are less than $\frac{1}{6}$[111], and thus a sufficiently large partial is situated in the centre, a stable configuration with three-fold symmetry may exist as for example some of the generalized splittings shown by Vítek and Kroupa (1969).

A number of sessile configurations have been proposed which have partial dislocations either on {110} planes alone (e.g. Kroupa and Vítek 1964) or on both {110} and {211} planes (e.g. Foxall *et al.* 1967, Duesbery

Downloaded by [University of Kiel] at 06:24 23 October 2014

and Hirsch 1968, Vítek and Kroupa 1968, Mitchell 1968). In these cases the Burgers vectors of the partials on {110} and {211} planes were $\frac{1}{8}\langle 110\rangle$ and $\frac{1}{6}\langle 111\rangle$ respectively. The core structure resulting from the present calculations could be regarded as a suitable amalgamation, possessing three-fold symmetry, of several of these splittings ; for example a variation on the configuration shown by Mitchell in his fig. 4 (*e*). The main differences are (i) partials on {211} planes have a much smaller Burgers vector than $\frac{1}{6}\langle 111\rangle$, (ii) no tendency towards a formation of partials with Burgers vectors parallel to $\langle 110\rangle$ was found, (iii) partials on {110} planes should be represented by a continuous distribution of partial dislocations and must lie on only one side of the centre for each plane.

In order to move the screw dislocation its core structure may have to be changed, for example, by an applied stress, into a glissile configuration. It could, however, move by direct jumps between stable configurations ; since the centre of the dislocation always coincides with a three-fold screw symmetry axis it follows that the only microscopic slip planes would then be {110} and {211} (these are the only planes connecting adjacent possible positions of the dislocation centre, as seen in fig. 1). Most of the displacement is concentrated on the three {110} planes radiating from the centre, which suggests that {110} planes will be the predominant slip planes in b.c.c. metals. Slip on {211} planes, which will be easier in the twinning sense, will probably occur less frequently and will be more sensitive to the orientation of the effective stress ; but it will be responsible for the slip asymmetry. However, we should not draw definitive conclusions about the motion of screw dislocations from this static study ; it will be necessary to investigate the influence of an applied stress upon the core structure.

Acknowledgments

The authors would like to thank Professors P. B. Hirsch, F.R.S. and J. W. Christian, and Dr. R. Bullough for their encouragement, valuable discussions and comments on the manuscript, and Drs. G. Taylor and D. Veselý for their discussions. V.V. would like to thank the S.R.C. and I.C.I. for Fellowships ; D.K.B. would like to thank the S.R.C. for a Fellowship when at Oxford.

References

Born, M., and Huang, K., 1954, *Dynamical Theory of Crystal Lattices* (Oxford : Clarendon Press).

Bowen, D. K., Christian, J. W., and Taylor, G., 1967, *Can. J. Phys.*, **45**, 903.

Bullough, R., and Perrin, R. C., 1968 a, *Dislocation Dynamics*, edited by A. R. Rosenfield, G. T. Hahn, A. L. Bement and R. I. Jaffee (McGraw-Hill), p. 175 ; 1968 b, *Proc. R. Soc.* A, **305**, 541.

Byron, J. F., and Hull, D., 1967, *J. less common Metals*, **13**, 71.

Chang, R., 1967, *Phil. Mag.*, **16**, 1021.

Cohen, J. B., Hinton, R., Lay, K., and Sass, S., 1962, *Acta metall.*, **10**, 894.

Duesbery, M. S., 1969, *Phil. Mag.*, **19**, 501.

Duesbery, M. S., and Foxall, R. A., 1969, *Phil. Mag.*, **20**, 719.

Downloaded by [University of Kiel] at 06:24 23 October 2014

DUESBERY, M. S., and HIRSCH, P. B., 1968, *Dislocation Dynamics*, edited by A. R. Rosenfield, G. T. Hahn, A. L. Bement and R. I. Jaffee (McGraw-Hill), p. 57.
EICHLER, H., and PEGEL, B., 1969, *Phys. Stat. Sol.*, **35,** 333.
ESCAIG, B., 1966, *J. Phys., Paris*, **27,** C3–205.
FONTAINE, G., 1968, Thesis, University of Paris.
FOXALL, R. A., DUESBERY, M. S., and HIRSCH, P. B., 1967, *Can. J. Phys.*, **45,** 607.
FRANK, F. C., and NICHOLAS, J. F., 1953, *Phil. Mag.*, **44,** 1213.
GEHLEN, P. C., ROSENFIELD, A. R., and HAHN, G. T., 1969, Conference on Fundamental Aspects of Dislocation Theory, N.B.S., Washington.
GIBSON, J. B., GOLAND, A. N., MILGRAM, M., and VINEYARD, G. H., 1960, *Phys. Rev.*, **120,** 1229.
HIRSCH, P. B., 1960, *Fifth Internat. Congs. Crystallography*, Cambridge, p. 139.
JOHNSON, R. A., 1964, *Phys. Rev.* A, **134,** 1329.
KROUPA, F., and VÍTEK, V., 1964, *Czech. J. Phys.* B, **14,** 337 ; 1967, *Can. J. Phys.*, **45,** 945.
MITCHELL, T. E., 1968, *Phil. Mag.*, **17,** 1196.
MITCHELL, T. E., FOXALL, R. A., and HIRSCH, P. B., 1963, *Phil. Mag.*, **8,** 1895.
ŠESTÁK, B., and ZÁRUBOVÁ, N., 1965, *Phys. Stat. Sol.*, **10,** 239.
ŠESTÁK, B., ZÁRUBOVÁ, N., and SLÁDEK, V., 1967, *Can. J. Phys.*, **45,** 1031.
SLEESWYK, A. W., 1963, *Phil. Mag.*, **8,** 1467.
STATHAM, C. D., 1968, Thesis, University of Oxford.
STROH, A. N., 1958, *Phil. Mag.*, **3,** 625.
SUZUKI, H., 1968, *Dislocation Dynamics*, edited by A. R. Rosenfield, G. T. Hahn, A. L. Bement, and R. I. Jaffee (McGraw-Hill), p. 679.
TAOKA, T., TAKEUCHI, S., and FURUBAYASHI, E., 1964, *J. phys. Soc. Japan*, **19,** 701.
VÍTEK, V., 1968, *Phil. Mag.*, **18,** 773 ; 1970, *Ibid.*, **21,** June.
VÍTEK, V., and KROUPA, F., 1966, *Phys. Stat. Sol.*, **18,** 703 ; 1968, *Czech. J. Phys.* B, **18,** 464 ; 1969, *Phil. Mag.*, **19,** 265.

Downloaded by [University of Kiel] at 06:24 23 October 2014